# ReGS: Reference-based Controllable Scene Stylization with Gaussian Splatting

**Yiqun Mei*** **Jiacong Xu*** **Vishal M. Patel**
Johns Hopkins University
{ymei7,jxu155, vpatel36}@jhu.edu

## Abstract

Referenced-based scene stylization that edits the appearance based on a content-aligned reference image is an emerging research area. Starting with a pretrained neural radiance field (NeRF), existing methods typically learn a novel appearance that matches the given style. Despite their effectiveness, they inherently suffer from time-consuming volume rendering, and thus are impractical for many real-time applications. In this work, we propose ReGS, which adapts 3D Gaussian Splatting (3DGS) for reference-based stylization to enable real-time stylized view synthesis. Editing the appearance of a pretrained 3DGS is challenging as it uses *discrete* Gaussians as 3D representation, which tightly bind appearance with geometry. Simply optimizing the appearance as prior methods do is often insufficient for modeling continuous textures in the given reference image. To address this challenge, we propose a novel texture-guided control mechanism that adaptively adjusts local responsible Gaussians to a new geometric arrangement, serving for desired texture details. The proposed process is guided by texture clues for effective appearance editing, and regularized by scene depth for preserving original geometric structure. With these novel designs, we show ReGS can produce state-of-the-art stylization results that respect the reference texture while embracing real-time rendering speed for free-view navigation.

## 1 Introduction

Stylizing a 3D scene based on a 2D artwork is an active research area in both computer vision and graphics [1, 2, 3, 4, 5, 6, 7]. One important direction of stylization aims to precisely stylize the scene appearance based on a 2D content-aligned reference image drawn by users [10]. Such problem has numerous applications in digital art, film production and virtual reality. In the classical graphics pipeline, completing this task requires experienced 3D artists to manually create a UV texture map as input to the shader, a tedious process requiring professional knowledge, significant time, and effort.

Over the past decades, tremendous progress has been made in automatic scene stylization by leveraging view synthesis methods. While early attempts [1, 2, 12, 13] suffer from geometry errors of point clouds or meshes, more recent methods [9, 8, 3, 4, 5, 6, 7] rely on radiance field (NeRF) [14], a powerful implicit 3D representation, to deliver high-quality renditions that are perceptually similar to the reference image. A typical stylization workflow starts from a pretrained NeRF model of the target scene, followed by an appearance optimization phase to match the given style. The density function is always fixed to maintain the scene geometry [8, 9, 3, 10, 6] . Despite their promising results, NeRF-based approaches consume high training and rendering costs in order to obtain satisfactory results. Although some recent efforts make fast training possible [15, 16, 17, 18, 19, 20], the improvement in efficiency often comes at the price of degraded visual quality. Meanwhile, real-time rendering at inference time still remains challenging.

*Equal contribution

38th Conference on Neural Information Processing Systems (NeurIPS 2024).

 https://doi.org/10.52202/079017-0132

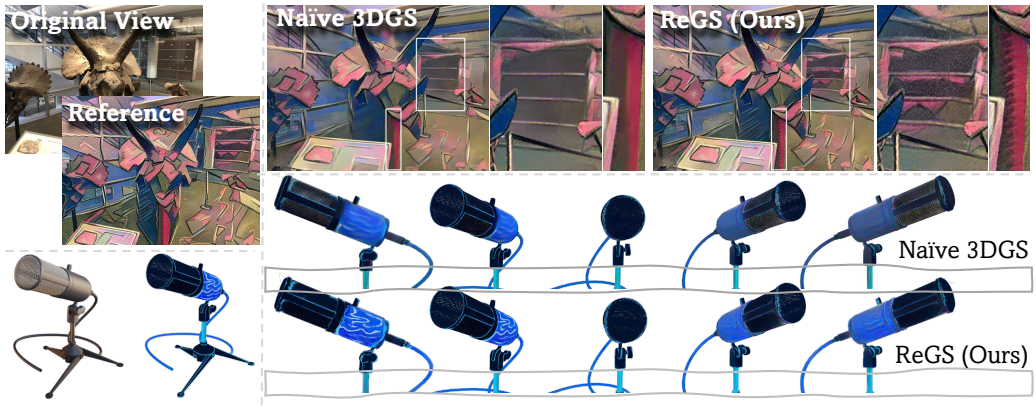


Figure 1: Given a pretrained 3DGS model of the target scene and its paired style reference, ReGS enables real-time stylized view synthesis (at 134 FPS) with high-fidelity texture well-aligned with the reference. In contrast, only optimizing the appearance of 3DGS (denoted as Naive 3DGS), as previous methods [8, 9, 3, 10, 6] do, fails to capture many texture details in the reference. We tackle the challenges in high-fidelity appearance editing with a texture-guided control mechanism that is significantly more effective than the default density control [11] in addressing texture underfitting. Side-by-side comparisons with default density control can be found in Figure 5.

Recently, 3D Gaussian Splatting (3DGS) [11] has become an emerging choice for representing 3D scenes. 3DGS creates millions of colored Gaussians with learnable attributes to jointly represent the target scene geometry and appearance. Importantly, it adopts splatting-based rasterization [21] to replace the time-consuming volume rendering of NeRF models, providing remarkably faster rendering speed while maintaining comparable visual quality. However, as it uses *discrete* 3D Gaussians to represent the reconstructed scene, optimizing their appearance with a fixed geometry layout (as NeRF-based methods do) is often inadequate to capture the *continuous* texture variance in the reference image. This "appearance-geometry entanglement" makes applying 3DGS to applications that require novel appearance, *i.e.* stylization, challenging. For 3DGS, how to properly control and edit the appearance without distorting the original geometry remains under-explored.

In this paper, we present a novel reference-based scene stylization method using 3DGS, dubbed ReGS, to enable real-time stylized view synthesis with high-fidelity textures well-aligned with the given reference. Similar to previous methods, our approach starts with a pretrained 3D Gaussian model of the target scene. The core enabler of ReGS is a novel texture-guided control procedure that makes high-fidelity appearance editing with ease. In particular, we adaptively adjust the local arrangement of responsible Gaussians in the appearance underfitting regions to a state that the desired textures specified in the reference image can be faithfully expressed. The control process is designed to **(1)** automatically identify target local Gaussians using texture clues, and **(2)** structurally distribute tiny Gaussians for fast detail infilling while **(3)** sticking to the original scene structure via a depth-based regularization. With these novel designs, ReGS is able to learn consistent 3D appearance that accurately follows the given reference image.

Following [10], we train ReGS on a set of pseudo-stylized images for view consistency, which are synthetic multi-view data created using extracted scene depth, alongside with a template-based matching loss to ensure style spread to the occluded regions. By combining these techniques with the proposed texture-guided control, ReGS is capable of producing visually appealing stylization results that attain both geometric and perceptual consistency. Through extensive experiments, we demonstrate that ReGS achieves state-of-the-art visual quality compared to existing stylization methods while enabling real-time view synthesis by embracing the fast rendering speed of Gaussian Splatting.

## 2 Related Work

### 2.1 3D Scene Representation

**Neural Radiance Field.** Reconstructing 3D scene from multi-view collections is a long-standing problem in computer vision. Early approaches adopting explicit mesh [22, 23, 24, 25] or voxel [26,

https://doi.org/10.52202/079017-0132

27, 28] based representations often suffer from geometry error and lack of appearance details [29]. Recent methods [30, 31, 32, 33, 34, 35] adopt learnable radiance fields [14] to capture 3D scene implicitly and outperform previous techniques by a large margin. However, NeRF models require millions of network queries for a single rendition that can be extremely time and resource-consuming. To reduce the training time, advanced methods adopt explicit/hybrid representations including voxel grid [18, 16, 15, 36, 37], octree [38, 39, 40], planes [41, 42, 17, 43] and hash grid [20], and successfully reduce the training time from days to minutes. Nevertheless, the rendering speed at inference time is still limited by their volumetric nature, which requires dense sampling along a ray to generate a single pixel.

**3D Gaussian Splatting**. Recently, 3D Gaussian Splatting (3DGS) [11] achieves real-time novel view synthesis based on a differentiable rasterizer [21] that efficiently projects millions of 3D Gaussians to a 2D canvas. Given its high efficiency, 3DGS becomes a promising solution to enable real-time vision applications, such as human avatar [44, 45, 46, 47], 3D object and immersive scene creation [48, 49, 50, 51], relighting [52, 53, 54, 55], surface or mesh reconstruction [56, 57], 3D segmentation [58, 59, 60], and SLAM [61, 62, 63]. Motivated by its high efficiency, our work explores 3DGS to enable real-time stylized view navigation.

### 2.2 2D Stylization

**Arbitrary Style Transfer.** Our method is related to the general 2D stylization [64], which transfers the style from an artwork to a target image while maintaining the original content structure. In the pioneering work, Gatys *et al*. [65] introduce an iterative scheme that progressively reduces the difference between the Gram statistics of generated image and style image features, yet lengthy optimization is required per style. To improve efficiency, later methods [66, 67, 68, 69, 70] focus on arbitrary image/video stylization by transferring the content image to target style spaces in a zero-shot manner. For example, Huang *et al*. [67] introduce AdaIN, which achieves real-time stylization by matching content features with the mean and standard deviation of style features. Linear style transfer [66] instead predicts a linear transformation matrix based on both content and style pairs. For video stylization, it is crucial to maintain temporal coherence of the stylized frames. Techniques [71, 72, 73, 74, 75, 76], such as flow-based wrapping [72], global SSIM constraint [75], and inter-frame feature similarity [76], are proposed to ensure the consistency.

**Optimization-based Style Transfer.** While arbitrary style transfer is desirable in terms of flexibility, they often fall short of reproducing small stylistic patterns and lack high-frequency details [8, 77]. Optimization-based Stylization [78, 79, 80, 81, 82, 77] is still the primary choice to ensure visual quality. For instance, a coarse-to-fine strategy is proposed by Liao *et al*. [82] to compute the nearest-neighbor field and build a semantically meaningful mapping between input and style images for visual attribute transfer. Kolkin *et al*. [77] reach state-of-the-art stylization quality by replacing the content features with the nearest style feature. To enable better controllability, example-based methods [83, 84, 85, 86] perform wrapping or stylizing based on the aligned correspondences between the style reference and content images. However, their 2D alignment is generally unsuitable for 3D scenes due to occlusions, leading to flickering effects [10].

### 2.3 3D Stylization

3D scene stylization extends artistic works beyond the 2D canvas [87]. To stylizing a 3D scene, both image exemplar [8, 9, 4] and text instructions [88, 89, 90, 91] have been explored as style guidance. This work focuses on image-exemplar-based methods. Early works [1, 2] typically back-project image colors as 3D point cloud for processing, and project stylized point features back to 2D for view synthesis. Yet, using point cloud often fails to represent complicated geometry and produces artifacts for complex scenes [8].

Benefiting from NeRF, methods stylizing radiance fields [9, 8, 3, 4, 5, 6, 7] have shown visually compelling and geometry-consistent results than previously possible. Similar to image stylization, several works [9, 3, 6, 7] deal with arbitrary or multiple style transfer using various techniques such as 2D-3D mutual learning [3], deferred style transformation [9], and hypernetwork [6]. While a universal stylizer might be desirable, these methods can only transfer the overall color tone and lack detailed style patterns, *i.e*. brushstrokes. Per-style optimization is still required for better visual quality. Among these methods [4, 8, 5, 92], ARF [8] shows state-of-the-art stylization capability


https://doi.org/10.52202/079017-0132

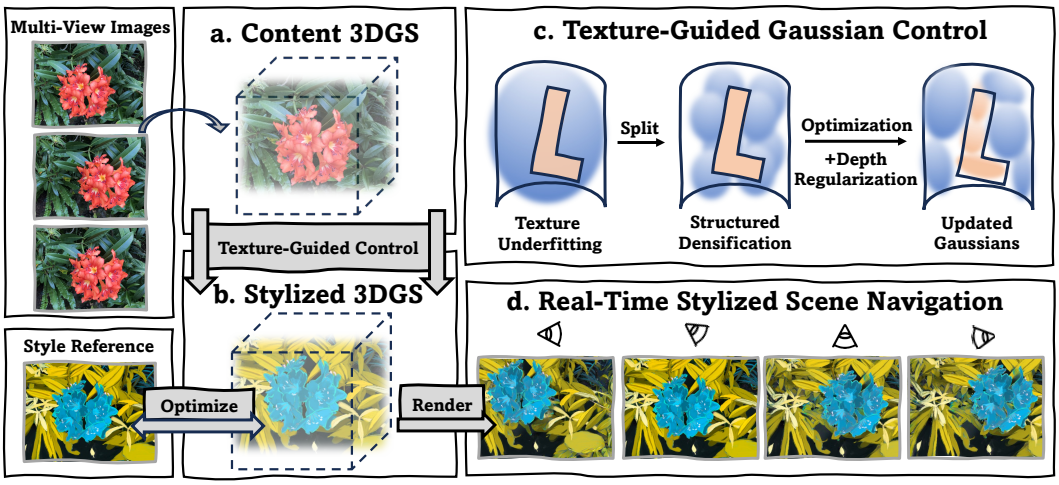


Figure 2: **An overview of ReGS**. (a) The proposed method starts with a pretrained content 3DGS of the target scene, and (b) outputs a stylized 3DGS that follows the reference. (c) We propose Texture-Guided Gaussian Control that can progressively resolve texture underfitting by automatically locating responsible Gaussians and adjusting local geometry layout for fitting high-frequency textures. (d) Once training is done, our method enables real-time stylized scene navigation.

by progressively matching the generated features with the closest style feature via nearest neighbor search. Besides NeRF-based approaches, concurrent works [93, 94, 95, 96] also explore 3DGS [11] as scene representation. However, these methods are designed for transferring styles from an arbitrary reference and lack controllability over generated results. To this end, Ref-NPR [10] introduces a reference-based scheme that controls stylized appearance based on a content-aligned reference image. Our work also focuses on this setting.

## 3 Method

An overview of ReGS is shown in Figure 2. ReGS takes a pretrained 3DGS model (Figure 2 (a)) of the target scene as well as a content-aligned reference image as inputs. It outputs a stylized 3DGS model (Figure 2 (b)) that bakes the texture of the reference image into the scene and enables real-time stylized views synthesis (Figure 2 (d)).

As 3DGS represents a scene as discrete Gaussians, simply optimizing its appearance often cannot capture the continuous texture details in the reference image. We introduce a texture-guided control mechanism to progressively address this challenge (Sec. 3.2). To ensure no geometry distortion happens during optimization, we propose a geometry regularization using scene depth (Sec. 3.3). We then introduce two techniques to encourage perceptual-consistent renditions (Sec. 3.4). Finally, we describe our training objectives in Sec. 3.5.

### 3.1 Preliminary: 3D Gaussian Splatting

Before introducing our method, we first provide a brief review of 3D Gaussian Splatting [11]. 3DGS represents the scene explicitly by a collection of learnable Gaussians. Each 3D Gaussian is attributed by a positional vector $\mu \in \mathbb{R}^3$ and a 3D covariance matrix $\mathbf{\Sigma} \in \mathbb{R}^{3\times3}$. Its influence on a space point $\mathbf{x}$ is proportional to a Gaussian distribution:

$$G(\mathbf{x}) = e^{-\frac{1}{2}(\mathbf{x}-\mu)^\top \mathbf{\Sigma}^{-1}(\mathbf{x}-\mu)}. \tag{1}$$

By definition, the covariance matrix should be positive semi-definite. This is achieved by decomposing $\mathbf{\Sigma}$ into a scaling matrix $\mathbf{S}$ and a quaternion $\mathbf{R}$ *i.e.* $\mathbf{\Sigma} = \mathbf{RSS}^\top\mathbf{R}^\top$. Each Gaussian also stores an opacity value $\alpha_i$ and a view-dependent color represented by Spherical Harmonic (SH) coefficients.

The rendering procedure is implemented as splatting-based rasterization [21] which projects Gaussians to a 2D canvas. The projected 2D splats are then sorted based on the depth to the camera. After


(a) Rendered depth images (b) Synthesized pseudo views

Figure 3: Examples of (a) rendered depth maps using Eq.3 and (b) synthesized stylized pseudo views.

sorting, the final color for each pixel is computed through $\alpha$-blending:

$$C = \sum_{i=1}^{n} c_i \alpha'_i \prod_{j=1}^{i-1} (1 - \alpha'_j), \tag{2}$$

where $c_i$ is a view-dependent color of the $i$-th Gaussian computed from SH. $\alpha'_i$ is the multiplication result of the learned opacity $\alpha_i$ and evaluated value of the projected 2D Gaussian.

During optimization, heuristic controls are employed to adaptively manage the density of Gaussians to better represent the scene. Specifically, it densifies Gaussians with large positional gradients to capture missing geometry and prunes Gaussians with small opacity to improve compactness.

### 3.2 Texture-Guided Gaussian Control

As a discrete scene representation, the geometry layout and arrangement of Gaussians essentially limit the range of appearance it can express. For example, as shown in Figure 2 (c), appearance underfitting happens frequently at the area where local granularity of Gaussians is greater than the variance of the texture, *e.g.* a smooth colored surface in the original scene is painted with rich details in the reference view. ReGS addresses such challenges via a novel texture-guided control that splits these responsible local Gaussians into a denser set suitable for high-frequency texture. Specifically, the proposed mechanism automatically identifies responsible Gaussians using texture clues and structurally replaces them with a denser set of tiny Gaussians to compensate for the missing details. We describe important designs of the proposed algorithm below.

**Texture Guidance.** The control algorithm is directly guided by texture clues. Specifically, we accumulate color gradients of all Gaussians over iterations and select Gaussians with larger gradient magnitude than a threshold for densification. We found that a larger color gradient corresponds to Gaussians that have large texture errors while the optimization struggles to find the correct colors to reduce the loss. This control scheme shares a similar spirit with the original control scheme in 3DGS, where they leverage positional gradients to locate Gaussians responsible for missing geometric features. But in stylization, scene geometry is already well-reconstructed through pretraining, and therefore, the positional gradient is no longer informative. As demonstrated in Figure 5, our color-based control scheme is more sensitive for pinpointing Gaussians with missing textures than the positional-based solution. In practical implementation, we increase density based on the gradient statistics of every 100 iterations.

**Structured Densification.** Traditional mesh subdivision [97] cuts large faces into more sub-faces to express surface details. Sharing a similar spirit, we structurally split each responsible Gaussians into a structured denser set to better represent texture details. Intuitively, after densification, newly added Gaussians need to approximate the original space coverage to avoid inducing large geometry errors, and they should be sufficiently small and form a dense set to capture appearance variance. Based on these considerations, we propose a structured densification scheme that adds tiny Gaussians into the most representative locations surrounding their parent Gaussian. Specifically, we use nine tiny Gaussians to replace a parent Gaussian. Eight of them correspond to eight separate octants divided by the equatorial plane and perpendicular meridian planes of the original ellipsoid. And the rest is placed at the original center. We reduce their size by shrinking the scales with a factor of 8 and copy remaining parameters from their parent Gaussian. We empirically found this setup can roughly maintain a space coverage that approximates the original geometry. As optimization continues, the densified Gaussians are progressively updated to infill missing textures.


https://doi.org/10.52202/079017-0132

### 3.3 Depth-based Geometry Regularization

While our control mechanism progressively improves texture details, it is essential to ensure the original scene geometry is preserved after optimization. We resort to the scene depth as an additional regularization to penalize geometry changes. Examples of rendered depth are shown in Figure 3 (a). Formally, we derive the scene depth via a $\alpha$-blending-based equation:

$$d = \sum_{i=1}^{n} d_i \alpha_i' \prod_{j=1}^{i-1} (1 - \alpha_j'), \tag{3}$$

where the $d_i$ is the z-buffer associated with the $i$th Gaussian and $\alpha_i{}'$ is the same evaluated opacity in Eq. 2. $d_i$ is computed by projecting the 3D location $\mu$ to the camera space.

The depth regularization is defined as the $L_1$ distance between a depth image $D_i$ rendered from original scene model $\mathbf{m}$ and a depth image $\widehat{D}_i$ rendered from the stylized model $\widehat{\mathbf{m}}$ using the same camera pose $\phi_i$ *i.e.* $\mathcal{L}_{depth} = \|\widehat{D}_i - D_i\|_1$.

### 3.4 View-Consistent Stylization

For stylization, it is necessary to ensure the stylized appearance is consistent across different viewpoints and inpaints the occluded areas. Following [10], we adopt two strategies to address them.

**Stylized Pseudo View Supervision.** An image with paired depth contains sufficient information to re-render from nearby viewpoints [98]. This allows us to create a set of stylized pseudo views for obtaining additional supervision from the reference image. Our synthesis approach is very similar to classic depth-based 3D warping [98, 99]. Specifically, we back-project the reference image $S_R$ to the world space using the depth image $D_R$ and its camera pose $\phi_R$. Then, we re-project these 3D points back to a new viewpoint $\phi_i$. The resulting 2D image $S_i$ is used as an additional style supervision. Examples of the created pseudo views are shown in Figure 3 (b). It is important to make sure supervision only happens on meaningful pixels, *i.e.* they are projections of 3D points that are visible from the current viewpoint $\phi_i$. Therefore, we conduct a visibility check by comparing the depth between the 2D projections of the 3D points and the depth image $D_i$ from the current viewpoint $\phi_i$. This results in a visibility mask $M_i$. Given the pseudo views and visibility masks, one can define a pseudo view supervision loss as

$$\mathcal{L}_{view} = \frac{1}{\|M_i\|_0} \|M_i \widehat{S}_i - M_i S_i\|_1, \tag{4}$$

where $\|.\|_0$ is the $\ell_0$-norm that counts the number of valid pixels and $\widehat{S}_i$ is renderings of the stylized model $\widehat{\mathbf{m}}$.

**Template Correspondence Matching (TCM) Loss.** To ensure stylized appearance spreads to the occluded areas, we adopt the same TCM loss proposed in [10]. We briefly describe it here and refer readers to [10] for more details. TCM regularizes the difference of semantic correspondences before and after stylization. Given the style reference $S_R$, its corresponding view $I_R$, and a scene image $I_i$ rendered from a camera pose $\phi_i$, it constructs a guidance feature $F_G$ by $F_{G_i}^{(x,y)} = F_{S_R}^{(x^*,y^*)}$ where

$$(x^*, y^*) = \underset{x',y'}{\operatorname{argmin}} \, \textbf{dist}(F_{I_i}^{(x,y)}, F_{I_R}^{(x',y')}). \tag{5}$$

Here, $F_{S_R}$, $F_{I_R}$, $F_{I_i}$ denote deep semantic features of image $S_R$, $I_R$, and $I_i$ extracted by an ImageNet pretrained VGG [100]. The superscript $(x, y)$ denotes the $xy$ coordinates on the feature map. **dist** denotes the cosine distance. After obtaining the guidance feature, TCM loss is defined as a cosine distance loss:

$$\mathcal{L}_{TCM} = \textbf{dist}(F_{\widehat{s}_i}, F_{G_i}), \tag{6}$$

where $F_{\widehat{s}_i}$ is the extracted VGG features of the generated stylized view $\widehat{S}_i$.

### 3.5 Training Objectives

Besides aforementioned depth loss $\mathcal{L}_{depth}$, pseudo view supervision loss $\mathcal{L}_{view}$ and TCM loss $\mathcal{L}_{TCM}$, ReGS further optimizes a reconstruction loss $\mathcal{L}_{rec}$ and a coarse color-matching loss $\mathcal{L}_{color}$ [10]. The reconstruction loss is defined as the $L_1$ distance between the reference $S_R$ and the corresponding

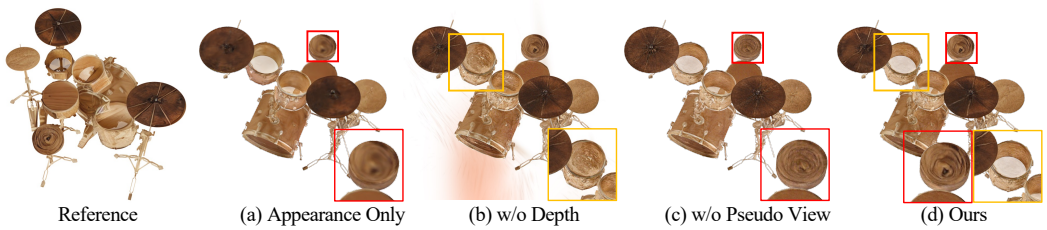


Figure 4: **Ablation study on different components of ReGS**. (a) Optimizing only the appearance of a 3DGS model cannot reproduce texture details. (b) Removing depth regularization causes Gaussians to float out from the surface and distort the origin geometry. (c) Without pseudo-view supervision, results lack view consistency. (d) Our full model produces the best results that faithfully respect the texture in the reference.

stylized output $\hat{S}_R$ to enforce appearance baking. The color-matching loss is defined as

$$\mathcal{L}_{color} = \|\widehat{S}_i^{(x,y)} - S_R^{(x^*,y^*)}\|_2^2, \tag{7}$$

where $S^{(x,y)}$ denotes the average color of a patch associated with feature-level index $(x, y)$. Feature-level index is computed using Eq. 9. This loss is directly adapted from [10] to encourage overall color matching in the occluded area. The overall loss for ReGS can be expressed as

$$\mathcal{L} = \lambda_{rec}\mathcal{L}_{rec} + \lambda_{depth}\mathcal{L}_{depth} + \lambda_{view}\mathcal{L}_{view} + \lambda_{tcm}\mathcal{L}_{TCM} + \lambda_{color}\mathcal{L}_{color} \tag{8}$$

where $\lambda_{(.)}$ denotes the balancing parameter.

### 3.6 Implementation and Training Details

ReGS uses 3D Gaussians [11] as the scene representation and is built upon their official codebase. We follow the default parameter settings to obtain the pretrained 3D Gaussian model of the photo-realistic scene. For stylization, as we do not expect view-dependent effects, we discard the higher order SH and only render diffuse color in the stylization phase. Therefore, content images used in $\mathcal{L}_{TCM}$ and $\mathcal{L}_{color}$ are the results of this diffuse model.

For texture-guided control, we start accumulating gradients after a warm-up of 100 iterations and then perform the densification operation based on the color gradient statistics of every 100 iterations. The control process stops when it reaches half of the total iterations. The gradient threshold is empirically set to $1e-5$ at the beginning, and we linearly reduce it to $5e-6$ to allow for refining tiny details in the later training stage. Following [10, 8], we use the ImageNet pretrained VGG16 [100] as the feature extractor and use the features produced by *relu*_3 and *relu*_4 in $\mathcal{L}_{TCM}$. For balancing parameters we set $\lambda_{rec} = \lambda_{tcm} = 1$, $\lambda_{depth} = 10$, $\lambda_{view} = 2$, and $\lambda_{color} = 15$, which are determined by a simple grid search on Blender [14] scenes. At each iteration, we always sample two views: the reference view and a random view. We train our model for 3000 iterations. The proposed method is implemented using PyTorch and trained on one A5000 GPU.

## 4 Experiments

In this section, we demonstrate the stylization quality and our designs through extensive experiments. More experiment results and ablations can be found in the supplemental file and accompanied video.

### 4.1 Datasets

The only available reference-based stylization dataset is provided by [10]. The dataset contains 12 selected scenes from Blender [14], LLFF [101], and Tanks and Temples [102]. Each scene is paired with a content-aligned reference image.

### 4.2 Ablation Study

We conduct controlled experiments to analyze the effectiveness of each design choice in ReGS. Results are illustrated in Figures 4 & 5. As illustrated in Figure 4, replacing any components of ReGS will harm the stylization quality. For example, Figure 4 (a) shows that optimizing only the


https://doi.org/10.52202/079017-0132

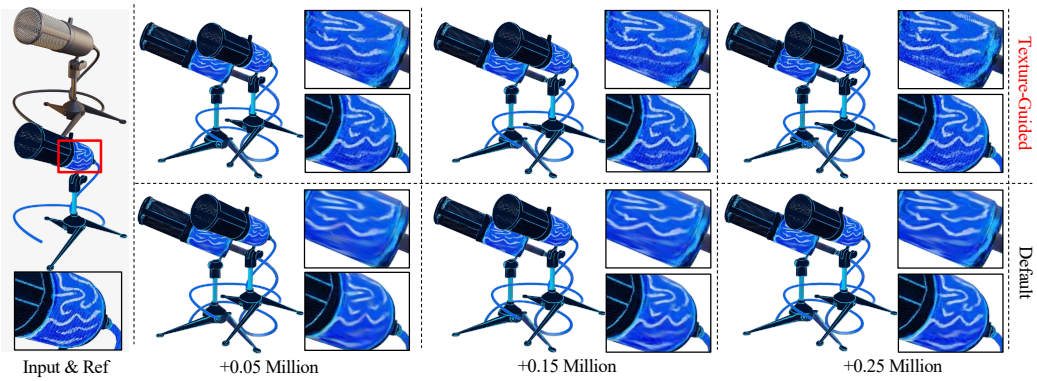


Figure 5: **Effectiveness of Texture-Guided Control.** We conduct controlled experiments by limiting the number of newly densified Gaussians throughout optimization. The pretrained model contains 0.3M Gaussians. The proposed texture-guided control can more faithfully reproduce the target texture details with a small number of Gaussians added (0.05M). The default strategy struggles to capture high-frequency details, even with a large number of Gaussians added (0.25M).

appearance with fixed geometry arrangement like previous methods [8, 6, 3, 9, 10] do fails to recover the texture details. As shown in Figure 4 (b), after removing depth regularization, Gaussians float out from the surface and distort the original scene geometry. Similarly, discarding the pseudo view supervision will induce view-inconsistency as highlighted in the inset (Figure 4 (c)). The full model overcomes these issues and produces more visually appealing results that follow the given reference.

**Effectiveness of Texture-Guided Control.** The core enabler of ReGS is the proposed texture-guided control mechanism that makes high-fidelity appearance editing with ease. Here, we demonstrate its effectiveness by comparing it with the default positional-gradient-guided density control [11] in addressing texture underfitting. Specifically, we conduct controlled experiments by setting a series of limits on the total number of Gaussians that can grow throughout optimization. Results are reported in Figure 5. One can see that by growing a very small amount of Gaussians (0.05M), the proposed texture-guided method can quickly infill most of the missing details. With more Gaussians added, it can further faithfully reproduce the given texture. In contrast, even with a large amount of new Gaussians (0.25M) created, the default method can barely capture high-frequency texture details. This is mainly because positional gradient is not sensitive to texture errors. As such, it fails to grow Gaussians in the regions with texture underfitting. And further moving these incorrectly placed Gaussians to the correct place for texture infilling is challenging. These results demonstrate our method is indeed more favorable for addressing appearance underfitting. Study on individual component (*i.e.* structured densification and color-gradient guidance) can be found in the supplement.

Table 1: Quantitative comparison of different stylization methods.

| Metric | ARF [8] | SNeRF [4] | Ref-NPR [10] | ReGS (Ours) |
|---|---|---|---|---|
| Ref-LPIPS↓ | 0.394 | 0.405 | 0.339 | **0.202** |
| Robustness↑ | 26.34 | 26.03 | 28.11 | **31.27** |
| Speed (fps) | 16.5 | 16.3 | 16.4 | **91.4** |

### 4.3 Compare with State-of-the-art Methods

To evaluate stylization performance, we compare our method with three state-of-the-art baselines: ARF [8], SNeRF [4], and Ref-NPR [10]. ARF [8] and SNeRF [4] are general stylization methods that conduct style transfer without considering content correspondence. Ref-NPR [10] is a reference-based stylization method similar to ours that aims to precisely edit the 3D appearance based on the reference. All baselines are NeRF-based approaches built upon Plenoxels [15].

**Qualitative Evaluation.** We report qualitative results in Figure 6. As shown, ARF [8] and SNeRF [4] cannot generate semantic-consistent results with respect to the reference image as they ignore content correspondence. In contrast, Ref-NPR [10] produces more controllable results but yields artifacts. In some challenging cases (*e.g.* last row in Figure 6), it also fails to achieve semantic consistent

https://doi.org/10.52202/079017-0132

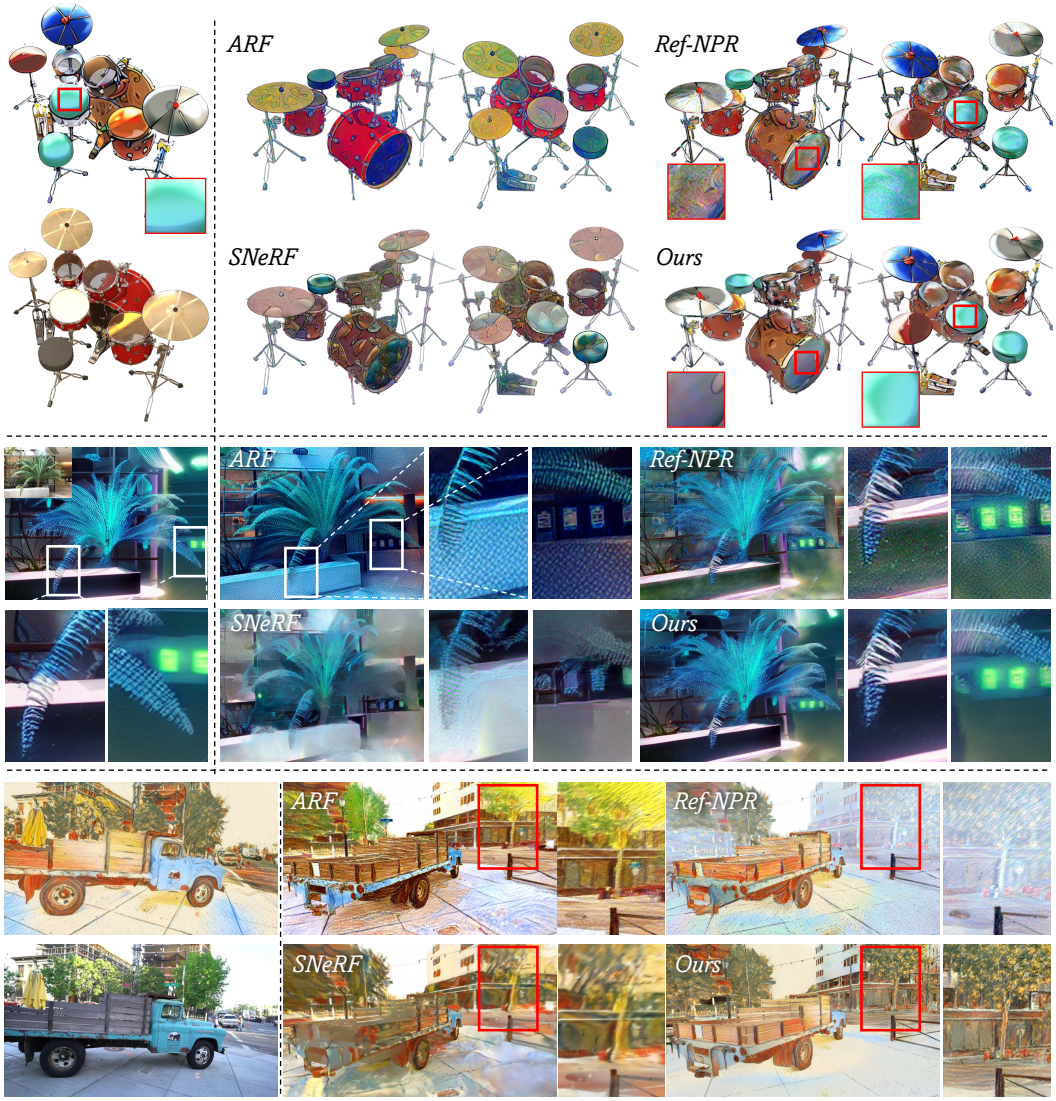


Figure 6: **Visual comparisons with state-of-the-art methods.** Paired reference and content view are shown on the left. Our method produces visual-compelling results that precisely follow the texture of the given reference, including the challenging high-frequency details such as the leaf in the second example. Baseline methods [10, 8, 4] either lack semantic consistency or produce artifacts.

stylization (*i.e.* green tree in the reference image is colored as white). In contrast, our method achieves better results that reproduce the desired texture, including challenging high-frequency ones.

**Quantitative Evaluation.** We present quantitative results in Table 1. Results are averaged over all scenes. We follow the protocol from [10] and report Ref-LPIPS and Robustness. Ref-LPIPS computes LPIPS [103] score between the reference image and the 10 nearest test views. To calculate robustness, we first (1) train a stylized base model $m_b$ and use it to render a set of stylized views as new references; (2) then we use these references to train another set of stylized models and (3) compute PSNR results between images produced by them and $m_b$ (using the same camera path). To measure run-time efficiency, we also report run-time FPS on a single A5000 GPU. As shown in Table 1, our method achieves the best results in terms of both quality and efficiency. Notably, our method enables real-time stylized view synthesis at 91 FPS.


https://doi.org/10.52202/079017-0132

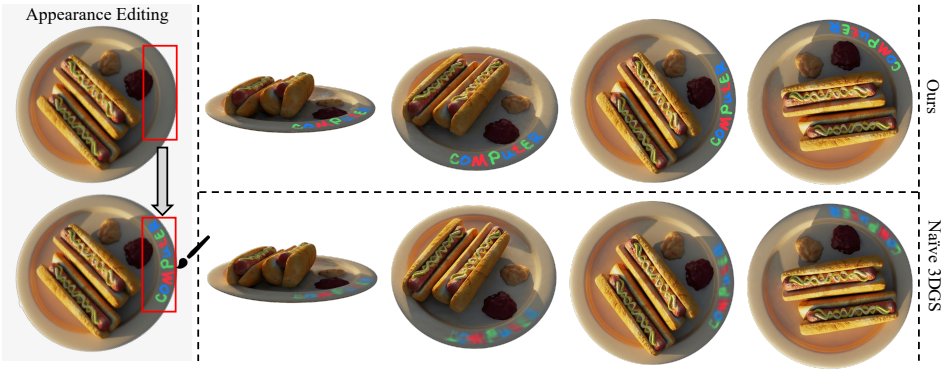


Figure 7: **Application: appearance editing.** Given a pretrained 3DGS model, our method allows users to make 3D appearance editing with ease by drawing on a 2D rendered view. Unlike NeRFs [14], just optimizing the appearance of a 3DGS model cannot robustly handle user edits.

## 5 Application: Appearance Editing

ReGS naturally enables high-fidelity appearance editing. As shown in Figure 7, given a pretrained 3DGS model and its rendering, our method allows users to make freehand edits on the image (*e.g.* "computer" on the plate) and robustly bake the edits back into the 3D scene with view-consistency. Unlike NeRFs [14], such task cannot be robustly handled by just optimizing the appearance of 3DGS (denoted as Naive Gaussian), especially when edits happen on a smooth surface where the granularity of Gaussians is greater than the texture variance. Benefiting from texture-guided control, our method can effectively locate these large Gaussians and replace them with a denser set for better appearance editing.

## 6 Conclusion

In this work, we introduce ReGS, which adapts Gaussian Splatting for reference-based controllable scene stylization. ReGS adopts a novel texture-guided control mechanism to make high-fidelity appearance editing with ease. This is achieved by adaptively replacing responsible Gaussians with a denser set to express the desired appearance details. The control process is guided by texture clues for appearance editing while preserving original scene geometry through a depth-based regularization. We demonstrate the state-of-the-art scene stylization quality and effective designs of ReGS through extensive experiments. Benefiting from the high efficiency of 3DGS, our method naturally enables real-time stylized view synthesis. Discussions of limitations can be found in the supplemental file.

## 7 Acknowledgment

This research is based upon work supported by the Office of the Director of National Intelligence (ODNI), Intelligence Advanced Research Projects Activity (IARPA), via IARPA R&D Contract No. 140D0423C0076. The views and conclusions contained herein are those of the authors and should not be interpreted as necessarily representing the official policies or endorsements, either expressed or implied, of the ODNI, IARPA, or the U.S. Government. The U.S. Government is authorized to reproduce and distribute reprints for Governmental purposes notwithstanding any copyright annotation thereon.

## References

[1] Hsin-Ping Huang, Hung-Yu Tseng, Saurabh Saini, Maneesh Singh, and Ming-Hsuan Yang. Learning to stylize novel views. In *ICCV*, pages 13869–13878, 2021.

[2] Fangzhou Mu, Jian Wang, Yicheng Wu, and Yin Li. 3d photo stylization: Learning to generate stylized novel views from a single image. In *CVPR*, pages 16273–16282, 2022.

[3] Yi-Hua Huang, Yue He, Yu-Jie Yuan, Yu-Kun Lai, and Lin Gao. Stylizednerf: consistent 3d scene stylization as stylized nerf via 2d-3d mutual learning. In *CVPR*, pages 18342–18352, 2022.

[4] Thu Nguyen-Phuoc, Feng Liu, and Lei Xiao. Snerf: stylized neural implicit representations for 3d scenes. *ACM Transactions on Graphics (TOG)*, 41(4):1–11, 2022.

[5] Can Wang, Ruixiang Jiang, Menglei Chai, Mingming He, Dongdong Chen, and Jing Liao. Nerf-art: Text-driven neural radiance fields stylization. *IEEE Transactions on Visualization and Computer Graphics*, 2023.

[6] Pei-Ze Chiang, Meng-Shiun Tsai, Hung-Yu Tseng, Wei-Sheng Lai, and Wei-Chen Chiu. Stylizing 3d scene via implicit representation and hypernetwork. In *WACV*, pages 1475–1484, 2022.

[7] Zhiwen Fan, Yifan Jiang, Peihao Wang, Xinyu Gong, Dejia Xu, and Zhangyang Wang. Unified implicit neural stylization. In *ECCV*, pages 636–654. Springer, 2022.

[8] Kai Zhang, Nick Kolkin, Sai Bi, Fujun Luan, Zexiang Xu, Eli Shechtman, and Noah Snavely. Arf: Artistic radiance fields. In *ECCV*, pages 717–733. Springer, 2022.

[9] Kunhao Liu, Fangneng Zhan, Yiwen Chen, Jiahui Zhang, Yingchen Yu, Abdulmotaleb El Saddik, Shijian Lu, and Eric P Xing. Stylerf: Zero-shot 3d style transfer of neural radiance fields. In *CVPR*, pages 8338–8348, 2023.

[10] Yuechen Zhang, Zexin He, Jinbo Xing, Xufeng Yao, and Jiaya Jia. Ref-npr: Reference-based non-photorealistic radiance fields for controllable scene stylization. In *CVPR*, pages 4242–4251, 2023.

[11] Bernhard Kerbl, Georgios Kopanas, Thomas Leimkühler, and George Drettakis. 3d gaussian splatting for real-time radiance field rendering. *ACM Transactions on Graphics (ToG)*, 42(4):1–14, 2023.

[12] Lukas Höllein, Justin Johnson, and Matthias Nießner. Stylemesh: Style transfer for indoor 3d scene reconstructions. In *CVPR*, pages 6198–6208, 2022.

[13] Jakub Fišer, Ondřej Jamriška, Michal Lukáč, Eli Shechtman, Paul Asente, Jingwan Lu, and Daniel Sỳkora. Stylit: illumination-guided example-based stylization of 3d renderings. *ACM Transactions on Graphics (TOG)*, 35(4):1–11, 2016.

[14] Ben Mildenhall, Pratul P Srinivasan, Matthew Tancik, Jonathan T Barron, Ravi Ramamoorthi, and Ren Ng. Nerf: Representing scenes as neural radiance fields for view synthesis. *Communications of the ACM*, 65(1):99–106, 2021.

[15] Sara Fridovich-Keil, Alex Yu, Matthew Tancik, Qinhong Chen, Benjamin Recht, and Angjoo Kanazawa. Plenoxels: Radiance fields without neural networks. In *CVPR*, pages 5501–5510, 2022.

[16] Cheng Sun, Min Sun, and Hwann-Tzong Chen. Direct voxel grid optimization: Super-fast convergence for radiance fields reconstruction. In *CVPR*, pages 5459–5469, 2022.

[17] Anpei Chen, Zexiang Xu, Andreas Geiger, Jingyi Yu, and Hao Su. Tensorf: Tensorial radiance fields. In *ECCV*, pages 333–350. Springer, 2022.

[18] Lingjie Liu, Jiatao Gu, Kyaw Zaw Lin, Tat-Seng Chua, and Christian Theobalt. Neural sparse voxel fields. *Advances in Neural Information Processing Systems*, 33:15651–15663, 2020.

[19] David B Lindell, Julien NP Martel, and Gordon Wetzstein. Autoint: Automatic integration for fast neural volume rendering. In *CVPR*, pages 14556–14565, 2021.

[20] Thomas Müller, Alex Evans, Christoph Schied, and Alexander Keller. Instant neural graphics primitives with a multiresolution hash encoding. *ACM Transactions on Graphics (ToG)*, 41(4):1–15, 2022.

[21] Matthias Zwicker, Hanspeter Pfister, Jeroen Van Baar, and Markus Gross. Ewa volume splatting. In *Proceedings Visualization, 2001. VIS'01.*, pages 29–538. IEEE, 2001.

[22] Michael Waechter, Nils Moehrle, and Michael Goesele. Let there be color! large-scale texturing of 3d reconstructions. In *ECCV*, pages 836–850. Springer, 2014.

[23] PE DEBEC. Modeling and rendering architecture from photographs: A hybrid geometry-and image-based approach. In *Proc. SIGGRAPH'96*, 1996.

[24] Shichen Liu, Tianye Li, Weikai Chen, and Hao Li. Soft rasterizer: A differentiable renderer for image-based 3d reasoning. In *ICCV*, pages 7708–7717, 2019.

 https://doi.org/10.52202/079017-0132

[25] Renke Wang, Guimin Que, Shuo Chen, Xiang Li, Jun Li, and Jian Yang. Creative birds: Self-supervised single-view 3d style transfer. In *ICCV*, pages 8775–8784, 2023.

[26] Kiriakos N Kutulakos and Steven M Seitz. A theory of shape by space carving. *International journal of computer vision*, 38:199–218, 2000.

[27] Steven M Seitz and Charles R Dyer. Photorealistic scene reconstruction by voxel coloring. *International Journal of Computer Vision*, 35:151–173, 1999.

[28] Richard Szeliski and Polina Golland. Stereo matching with transparency and matting. In *ICCV*, pages 517–524. IEEE, 1998.

[29] Kyle Gao, Yina Gao, Hongjie He, Dening Lu, Linlin Xu, and Jonathan Li. Nerf: Neural radiance field in 3d vision, a comprehensive review. *arXiv preprint arXiv:2210.00379*, 2022.

[30] Jonathan T Barron, Ben Mildenhall, Matthew Tancik, Peter Hedman, Ricardo Martin-Brualla, and Pratul P Srinivasan. Mip-nerf: A multiscale representation for anti-aliasing neural radiance fields. In *ICCV*, pages 5855–5864, 2021.

[31] Jonathan T Barron, Ben Mildenhall, Dor Verbin, Pratul P Srinivasan, and Peter Hedman. Mip-nerf 360: Unbounded anti-aliased neural radiance fields. In *CVPR*, pages 5470–5479, 2022.

[32] Ricardo Martin-Brualla, Noha Radwan, Mehdi SM Sajjadi, Jonathan T Barron, Alexey Dosovitskiy, and Daniel Duckworth. Nerf in the wild: Neural radiance fields for unconstrained photo collections. In *CVPR*, pages 7210–7219, 2021.

[33] Alex Yu, Vickie Ye, Matthew Tancik, and Angjoo Kanazawa. pixelnerf: Neural radiance fields from one or few images. In *CVPR*, pages 4578–4587, 2021.

[34] Dor Verbin, Peter Hedman, Ben Mildenhall, Todd Zickler, Jonathan T Barron, and Pratul P Srinivasan. Ref-nerf: Structured view-dependent appearance for neural radiance fields. In *CVPR*, pages 5481–5490, 2022.

[35] Xin Huang, Qi Zhang, Ying Feng, Hongdong Li, Xuan Wang, and Qing Wang. Hdr-nerf: High dynamic range neural radiance fields. In *CVPR*, pages 18398–18408, 2022.

[36] Cheng Sun, Min Sun, and Hwann-Tzong Chen. Direct voxel grid optimization: Super-fast convergence for radiance fields reconstruction. In *CVPR*, pages 5459–5469, 2022.

[37] Peter Hedman, Pratul P Srinivasan, Ben Mildenhall, Jonathan T Barron, and Paul Debevec. Baking neural radiance fields for real-time view synthesis. In *ICCV*, pages 5875–5884, 2021.

[38] Alex Yu, Ruilong Li, Matthew Tancik, Hao Li, Ren Ng, and Angjoo Kanazawa. Plenoctrees for real-time rendering of neural radiance fields. In *ICCV*, pages 5752–5761, 2021.

[39] Liao Wang, Jiakai Zhang, Xinhang Liu, Fuqiang Zhao, Yanshun Zhang, Yingliang Zhang, Minye Wu, Jingyi Yu, and Lan Xu. Fourier plenoctrees for dynamic radiance field rendering in real-time. In *CVPR*, pages 13524–13534, 2022.

[40] Haotian Bai, Yiqi Lin, Yize Chen, and Lin Wang. Dynamic plenoctree for adaptive sampling refinement in explicit nerf. In *ICCV*, pages 8785–8795, 2023.

[41] Eric R Chan, Connor Z Lin, Matthew A Chan, Koki Nagano, Boxiao Pan, Shalini De Mello, Orazio Gallo, Leonidas J Guibas, Jonathan Tremblay, Sameh Khamis, et al. Efficient geometry-aware 3d generative adversarial networks. In *CVPR*, pages 16123–16133, 2022.

[42] Ang Cao and Justin Johnson. Hexplane: A fast representation for dynamic scenes. In *CVPR*, pages 130–141, 2023.

[43] Sara Fridovich-Keil, Giacomo Meanti, Frederik Rahbæk Warburg, Benjamin Recht, and Angjoo Kanazawa. K-planes: Explicit radiance fields in space, time, and appearance. In *CVPR*, pages 12479–12488, 2023.

[44] Liangxiao Hu, Hongwen Zhang, Yuxiang Zhang, Boyao Zhou, Boning Liu, Shengping Zhang, and Liqiang Nie. Gaussianavatar: Towards realistic human avatar modeling from a single video via animatable 3d gaussians. *arXiv preprint arXiv:2312.02134*, 2023.

[45] Zhe Li, Zerong Zheng, Lizhen Wang, and Yebin Liu. Animatable gaussians: Learning pose-dependent gaussian maps for high-fidelity human avatar modeling. *arXiv preprint arXiv:2311.16096*, 2023.

[46] Mengtian Li, Shengxiang Yao, Zhifeng Xie, Keyu Chen, and Yu-Gang Jiang. Gaussianbody: Clothed human reconstruction via 3d gaussian splatting. *arXiv preprint arXiv:2401.09720*, 2024.

[47] Muhammed Kocabas, Jen-Hao Rick Chang, James Gabriel, Oncel Tuzel, and Anurag Ranjan. Hugs: Human gaussian splats. *arXiv preprint arXiv:2311.17910*, 2023.

[48] Jiaxiang Tang, Jiawei Ren, Hang Zhou, Ziwei Liu, and Gang Zeng. Dreamgaussian: Generative gaussian splatting for efficient 3d content creation. In *ICLR*, 2024.

[49] Taoran Yi, Jiemin Fang, Guanjun Wu, Lingxi Xie, Xiaopeng Zhang, Wenyu Liu, Qi Tian, and Xinggang Wang. Gaussiandreamer: Fast generation from text to 3d gaussian splatting with point cloud priors. *arXiv preprint arXiv:2310.08529*, 2023.

[50] Jaeyoung Chung, Suyoung Lee, Hyeongjin Nam, Jaerin Lee, and Kyoung Mu Lee. Luciddreamer: Domain-free generation of 3d gaussian splatting scenes. *arXiv preprint arXiv:2311.13384*, 2023.

[51] Xian Liu, Xiaohang Zhan, Jiaxiang Tang, Ying Shan, Gang Zeng, Dahua Lin, Xihui Liu, and Ziwei Liu. Humangaussian: Text-driven 3d human generation with gaussian splatting. *arXiv preprint arXiv:2311.17061*, 2023.

[52] Jian Gao, Chun Gu, Youtian Lin, Hao Zhu, Xun Cao, Li Zhang, and Yao Yao. Relightable 3d gaussian: Real-time point cloud relighting with brdf decomposition and ray tracing. *arXiv preprint arXiv:2311.16043*, 2023.

[53] Shunsuke Saito, Gabriel Schwartz, Tomas Simon, Junxuan Li, and Giljoo Nam. Relightable gaussian codec avatars. *arXiv preprint arXiv:2312.03704*, 2023.

[54] Zhihao Liang, Qi Zhang, Ying Feng, Ying Shan, and Kui Jia. Gs-ir: 3d gaussian splatting for inverse rendering. *arXiv preprint arXiv:2311.16473*, 2023.

[55] Yahao Shi, Yanmin Wu, Chenming Wu, Xing Liu, Chen Zhao, Haocheng Feng, Jingtuo Liu, Liangjun Zhang, Jian Zhang, Bin Zhou, et al. Gir: 3d gaussian inverse rendering for relightable scene factorization. *arXiv preprint arXiv:2312.05133*, 2023.

[56] Antoine Guédon and Vincent Lepetit. Sugar: Surface-aligned gaussian splatting for efficient 3d mesh reconstruction and high-quality mesh rendering. *arXiv preprint arXiv:2311.12775*, 2023.

[57] Hanlin Chen, Chen Li, and Gim Hee Lee. Neusg: Neural implicit surface reconstruction with 3d gaussian splatting guidance. *arXiv preprint arXiv:2312.00846*, 2023.

[58] Shijie Zhou, Haoran Chang, Sicheng Jiang, Zhiwen Fan, Zehao Zhu, Dejia Xu, Pradyumna Chari, Suya You, Zhangyang Wang, and Achuta Kadambi. Feature 3dgs: Supercharging 3d gaussian splatting to enable distilled feature fields. *arXiv preprint arXiv:2312.03203*, 2023.

[59] Jiazhong Cen, Jiemin Fang, Chen Yang, Lingxi Xie, Xiaopeng Zhang, Wei Shen, and Qi Tian. Segment any 3d gaussians. *arXiv preprint arXiv:2312.00860*, 2023.

[60] Bin Dou, Tianyu Zhang, Yongjia Ma, Zhaohui Wang, and Zejian Yuan. Cosseggaussians: Compact and swift scene segmenting 3d gaussians. *arXiv preprint arXiv:2401.05925*, 2024.

[61] Vladimir Yugay, Yue Li, Theo Gevers, and Martin R Oswald. Gaussian-slam: Photo-realistic dense slam with gaussian splatting. *arXiv preprint arXiv:2312.10070*, 2023.

[62] Hidenobu Matsuki, Riku Murai, Paul HJ Kelly, and Andrew J Davison. Gaussian splatting slam. *arXiv preprint arXiv:2312.06741*, 2023.

[63] Mingrui Li, Shuhong Liu, and Heng Zhou. Sgs-slam: Semantic gaussian splatting for neural dense slam. *arXiv preprint arXiv:2402.03246*, 2024.

[64] Yongcheng Jing, Yezhou Yang, Zunlei Feng, Jingwen Ye, Yizhou Yu, and Mingli Song. Neural style transfer: A review. *IEEE transactions on visualization and computer graphics*, 26(11):3365–3385, 2019.

[65] Leon A Gatys, Alexander S Ecker, and Matthias Bethge. Image style transfer using convolutional neural networks. In *CVPR*, pages 2414–2423, 2016.

[66] Xueting Li, Sifei Liu, Jan Kautz, and Ming-Hsuan Yang. Learning linear transformations for fast image and video style transfer. In *CVPR*, pages 3809–3817, 2019.

[67] Xun Huang and Serge Belongie. Arbitrary style transfer in real-time with adaptive instance normalization. In *ICCV*, pages 1501–1510, 2017.

 https://doi.org/10.52202/079017-0132

[68] Songhua Liu, Tianwei Lin, Dongliang He, Fu Li, Meiling Wang, Xin Li, Zhengxing Sun, Qian Li, and Errui Ding. Adaattn: Revisit attention mechanism in arbitrary neural style transfer. In *ICCV*, pages 6649–6658, 2021.

[69] Dae Young Park and Kwang Hee Lee. Arbitrary style transfer with style-attentional networks. In *CVPR*, pages 5880–5888, 2019.

[70] Yongcheng Jing, Xiao Liu, Yukang Ding, Xinchao Wang, Errui Ding, Mingli Song, and Shilei Wen. Dynamic instance normalization for arbitrary style transfer. In *Proceedings of the AAAI conference on artificial intelligence*, volume 34, pages 4369–4376, 2020.

[71] Dongdong Chen, Jing Liao, Lu Yuan, Nenghai Yu, and Gang Hua. Coherent online video style transfer. In *ICCV*, pages 1105–1114, 2017.

[72] Haozhi Huang, Hao Wang, Wenhan Luo, Lin Ma, Wenhao Jiang, Xiaolong Zhu, Zhifeng Li, and Wei Liu. Real-time neural style transfer for videos. In *CVPR*, pages 783–791, 2017.

[73] Manuel Ruder, Alexey Dosovitskiy, and Thomas Brox. Artistic style transfer for videos and spherical images. *International Journal of Computer Vision*, 126(11):1199–1219, 2018.

[74] Wenjing Wang, Jizheng Xu, Li Zhang, Yue Wang, and Jiaying Liu. Consistent video style transfer via compound regularization. In *Proceedings of the AAAI conference on artificial intelligence*, volume 34, pages 12233–12240, 2020.

[75] Xinxiao Wu and Jialu Chen. Preserving global and local temporal consistency for arbitrary video style transfer. In *Proceedings of the 28th ACM International Conference on Multimedia*, pages 1791–1799, 2020.

[76] Yingying Deng, Fan Tang, Weiming Dong, Haibin Huang, Chongyang Ma, and Changsheng Xu. Arbitrary video style transfer via multi-channel correlation. In *Proceedings of the AAAI Conference on Artificial Intelligence*, volume 35, pages 1210–1217, 2021.

[77] Nicholas Kolkin, Michal Kucera, Sylvain Paris, Daniel Sykora, Eli Shechtman, and Greg Shakhnarovich. Neural neighbor style transfer. *arXiv e-prints*, pages arXiv–2203, 2022.

[78] Chuan Li and Michael Wand. Combining markov random fields and convolutional neural networks for image synthesis. In *CVPR*, pages 2479–2486, 2016.

[79] Eric Risser, Pierre Wilmot, and Connelly Barnes. Stable and controllable neural texture synthesis and style transfer using histogram losses. *arXiv preprint arXiv:1701.08893*, 2017.

[80] Shuyang Gu, Congliang Chen, Jing Liao, and Lu Yuan. Arbitrary style transfer with deep feature reshuffle. In *CVPR*, pages 8222–8231, 2018.

[81] Nicholas Kolkin, Jason Salavon, and Gregory Shakhnarovich. Style transfer by relaxed optimal transport and self-similarity. In *CVPR*, pages 10051–10060, 2019.

[82] Jing Liao, Yuan Yao, Lu Yuan, Gang Hua, and Sing Bing Kang. Visual atribute transfer through deep image analogy. *ACM Transactions on Graphics*, 36(4):120, 2017.

[83] Ondřej Jamriška, Šárka Sochorová, Ondřej Texler, Michal Lukáč, Jakub Fišer, Jingwan Lu, Eli Shechtman, and Daniel Sỳkora. Stylizing video by example. *ACM Transactions on Graphics (TOG)*, 38(4):1–11, 2019.

[84] Ahmed Selim, Mohamed Elgharib, and Linda Doyle. Painting style transfer for head portraits using convolutional neural networks. *ACM Transactions on Graphics (ToG)*, 35(4):1–18, 2016.

[85] YiChang Shih, Sylvain Paris, Connelly Barnes, William T Freeman, and Frédo Durand. Style transfer for headshot portraits. *ACM Transactions on Graphics*, 33(4):1–14, 2014.

[86] Ondřej Texler, David Futschik, Michal Kučera, Ondřej Jamriška, Šárka Sochorová, Menclei Chai, Sergey Tulyakov, and Daniel Sỳkora. Interactive video stylization using few-shot patch-based training. *ACM Transactions on Graphics (TOG)*, 39(4):73–1, 2020.

[87] Yingshu Chen, Guocheng Shao, Ka Chun Shum, Binh-Son Hua, and Sai-Kit Yeung. Advances in 3d neural stylization: A survey. *arXiv preprint arXiv:2311.18328*, 2023.

[88] Ayaan Haque, Matthew Tancik, Alexei A Efros, Aleksander Holynski, and Angjoo Kanazawa. Instruct-nerf2nerf: Editing 3d scenes with instructions. In *ICCV*, pages 19740–19750, 2023.

[89] Junjie Wang, Jiemin Fang, Xiaopeng Zhang, Lingxi Xie, and Qi Tian. Gaussianeditor: Editing 3d gaussians delicately with text instructions. In *CVPR*, pages 20902–20911, 2024.

[90] Yiwen Chen, Zilong Chen, Chi Zhang, Feng Wang, Xiaofeng Yang, Yikai Wang, Zhongang Cai, Lei Yang, Huaping Liu, and Guosheng Lin. Gaussianeditor: Swift and controllable 3d editing with gaussian splatting. In *CVPR*, pages 21476–21485, 2024.

[91] Jiemin Fang, Junjie Wang, Xiaopeng Zhang, Lingxi Xie, and Qi Tian. Gaussianeditor: Editing 3d gaussians delicately with text instructions. *arXiv preprint arXiv:2311.16037*, 2023.

[92] Zicheng Zhang, Yinglu Liu, Congying Han, Yingwei Pan, Tiande Guo, and Ting Yao. Transforming radiance field with lipschitz network for photorealistic 3d scene stylization. In *CVPR*, pages 20712–20721, 2023.

[93] Áron Samuel Kovács, Pedro Hermosilla, and Renata G Raidou. G-style: Stylized gaussian splatting. *arXiv preprint arXiv:2408.15695*, 2024.

[94] Kunhao Liu, Fangneng Zhan, Muyu Xu, Christian Theobalt, Ling Shao, and Shijian Lu. Stylegaussian: Instant 3d style transfer with gaussian splatting. *arXiv preprint arXiv:2403.07807*, 2024.

[95] Dingxi Zhang, Zhuoxun Chen, Yu-Jie Yuan, Fang-Lue Zhang, Zhenliang He, Shiguang Shan, and Lin Gao. Stylizedgs: Controllable stylization for 3d gaussian splatting. *arXiv preprint arXiv:2404.05220*, 2024.

[96] Abhishek Saroha, Mariia Gladkova, Cecilia Curreli, Tarun Yenamandra, and Daniel Cremers. Gaussian splatting in style. *arXiv preprint arXiv:2403.08498*, 2024.

[97] Denis Zorin, Peter Schröder, and Wim Sweldens. Interpolating subdivision for meshes with arbitrary topology. In *Proceedings of the 23rd annual conference on Computer graphics and interactive techniques*, pages 189–192, 1996.

[98] William R Mark, Leonard McMillan, and Gary Bishop. Post-rendering 3d warping. In *Proceedings of the 1997 symposium on Interactive 3D graphics*, pages 7–ff, 1997.

[99] Leonard McMillan and Gary Bishop. Plenoptic modeling: An image-based rendering system. In *Seminal Graphics Papers: Pushing the Boundaries, Volume 2*, pages 433–440. 2023.

[100] Karen Simonyan and Andrew Zisserman. Very deep convolutional networks for large-scale image recognition. *arXiv preprint arXiv:1409.1556*, 2014.

[101] Ben Mildenhall, Pratul P Srinivasan, Rodrigo Ortiz-Cayon, Nima Khademi Kalantari, Ravi Ramamoorthi, Ren Ng, and Abhishek Kar. Local light field fusion: Practical view synthesis with prescriptive sampling guidelines. *ACM Transactions on Graphics (TOG)*, 38(4):1–14, 2019.

[102] Arno Knapitsch, Jaesik Park, Qian-Yi Zhou, and Vladlen Koltun. Tanks and temples: Benchmarking large-scale scene reconstruction. *ACM Transactions on Graphics*, 36(4), 2017.

[103] Richard Zhang, Phillip Isola, Alexei A Efros, Eli Shechtman, and Oliver Wang. The unreasonable effectiveness of deep features as a perceptual metric. In *Proceedings of the IEEE conference on computer vision and pattern recognition*, pages 586–595, 2018.

[104] Chong Bao, Yinda Zhang, Bangbang Yang, Tianxing Fan, Zesong Yang, Hujun Bao, Guofeng Zhang, and Zhaopeng Cui. Sine: Semantic-driven image-based nerf editing with prior-guided editing field. In *CVPR*, pages 20919–20929, 2023.

[105] Can Wang, Ruixiang Jiang, Menglei Chai, Mingming He, Dongdong Chen, and Jing Liao. Nerf-art: Text-driven neural radiance fields stylization. *IEEE Transactions on Visualization and Computer Graphics*, 2023.

 https://doi.org/10.52202/079017-0132

# Supplemental Material

## A Video Demonstration

We encourage readers to watch the provided supplemental video for a better demonstration of the stylization quality of ReGS.

## B More Implementation Details

We describe additional implementation details here. As discussed in the main manuscript, our method adopts the TCM loss $\mathcal{L}_{TCM}$ and color-matching loss $\mathcal{L}_{color}$ to encourage stylization spread to occluded areas. Specifically, similar to [10], we use the standard TCM loss for the first 70% iterations. For the last 30% iterations, we replace the content feature matching (Eq. 5 in the main manuscript) with a style feature matching, *i.e.* matching between features of a generated stylized view $\widehat{S}_i$ and the reference image $S_R$. This results in an online stylization loss similar to NNFM [8]. Formally, we construct an online guidance feature $F_{G_i}$ by $F_{G_i}^{(x,y)} = F_{S_R}^{(x^*,y^*)}$ where

$$(x^*, y^*) = \underset{x',y'}{\operatorname{argmin}} \textbf{dist}(F_{\widehat{S}_i}^{(x,y)}, F_{S_R}^{(x',y')}). \tag{9}$$

where $F_{\widehat{S}_i}$ and $F_{S_R}$ denote the deep semantic features of a generated stylized view $\widehat{S}_i$ and the reference image $S_R$ extracted by an ImageNet pretrained VGG [100]. And the loss is still computed as the cosine distance between $F_{\widehat{S}_i}$ and $F_{G_i}$. We further remove the color matching loss at this phase. These techniques are shown to be useful for a smoother content update [10]. For appearance editing, training takes about 50 seconds. For spreading appearance to other views, training takes about 5-6 minutes for all scenes due to the costly TCM loss. Detailed algorithms can be found in Algorithm 12.

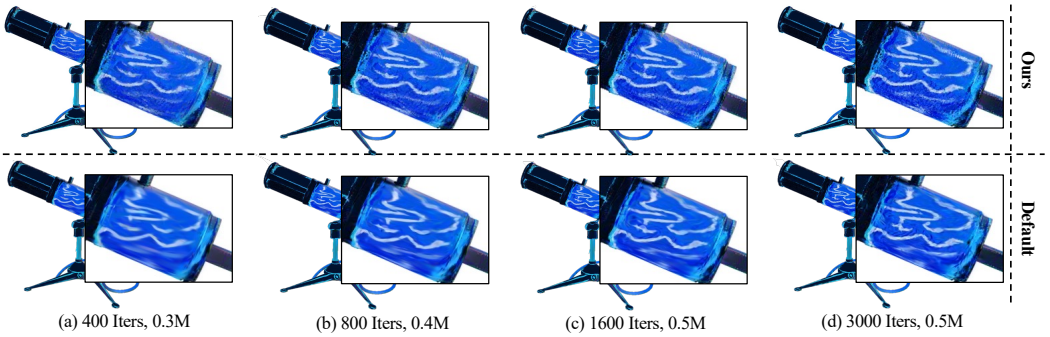


Figure 8: **Additional ablation study on structured densification.** Structured densification allows ReGS to create dense set of tiny Gaussians for representing high-frequency details. This enables our method to quickly infill the most of textures with a small amount of Gaussians tiny created ((a)). In contrast, the default strategy fails to express many details even with a large amount of Gaussians added ((d)).

## C Additional Ablation Study

### C.1 Structured Densification

Structured densification replaces a responsible Gaussian by a dense set of tiny Gaussians without inducing large geometry errors. Here we investigate its effectiveness by comparing it with the default replacement strategy in [11] that splits a parent Gaussian into two “medium-sized" Gaussians by shrinking with a scale factor of 1.6. Compared to their method, our approach creates a much denser set (9 vs. 2 added Gaussians) of much smaller (shrinking by 8 vs. 1.6) Gaussians in a structured way to replace the parent Gaussian. We report the comparison results in Figure 8. Each column corresponds to a snapshot at the noted iterations during training. Densification stops at the 1500 iteration. For fair comparison, we reduce the gradient threshold of the default strategy to ensure that densification creates a similar number of new Gaussians after each operation. Both methods are

https://doi.org/10.52202/079017-0132

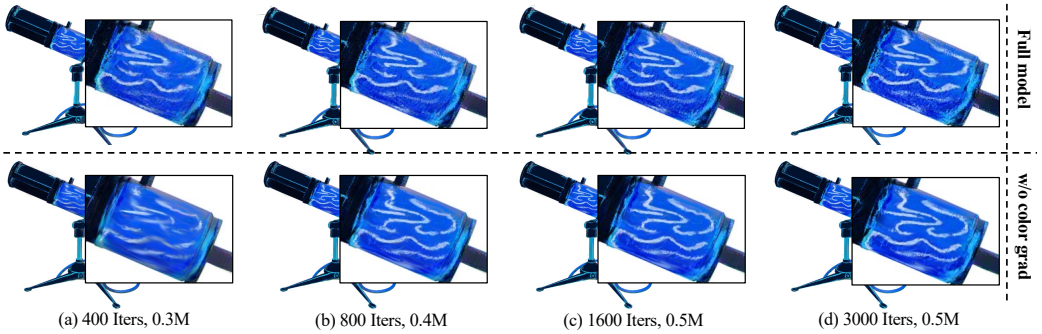


Figure 9: Ablation study on Texture Guidance (*i.e.* color-gradient guidance). Replacing texture guidance with positional-gradient guidance (bottom) fails to capture texture details.

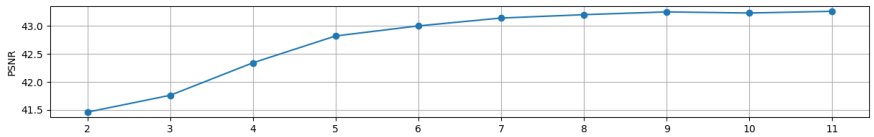


Figure 10: Ablation study on the number of Gaussians for each responsible Gaussian to be split. Small number cannot capture full details. Performance becomes saturated as the number grows.

based on the color-gradient-guided density control. As shown in Figure 8, the default strategy fails to express many details even after creating a large amount of Gaussians (*i.e.* Figure 8 (d)). This is mainly because the granularity of added Gaussians are not small enough to capture the high-frequency details. Therefore, their model has to repeatedly densify many times to reach a granularity that can match the texture variance. In contrast, benefiting from the structured densification, our method can quickly reproduce most of details by creating a small amount of tiny Gaussians, and shows much faster convergence. These results demonstrate the effectiveness of the proposed strategy in addressing texture underfitting.

### C.2 Texture (Color-Gradient) Guidance

Similarly, here we conduct an ablation study on color-gradient guidance. We construct the baseline by removing texture guidance from the full model (i.e., switching to the default positional-gradient guidance). We report the results in Figure 9. As shown, without texture guidance, the model fails to capture tiny texture details in the reference.

### C.3 Densification Number

Structured desertification splits a large Gaussian into a set of small Gaussians to infill the missing texture. Here we conduct an ablation study on the number of Gaussians for each responsible Gaussian to be split and present results in Figure 10. We plot the PSNR value between the style reference and the corresponding stylized view to quantitatively show the texture fitting capability using Blender scenes. As shown, when the number is small, the model fails to capture the target texture details. As this number grows, the performance becomes saturated. When the number equals 9, the model can

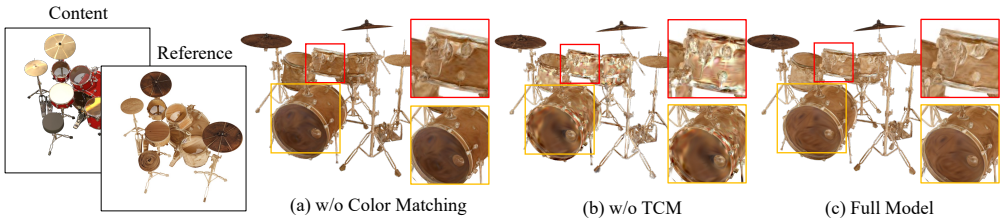


Figure 11: Ablation study on adopted TCM and color matching loss. Removing color matching loss leads to color mismatch and removing TCM leads to artifacts in occluded areas.


https://doi.org/10.52202/079017-0132

**Algorithm 1: Texture-Guided Control**

**Input:** $\mathcal{G} = \{G_i(\mu_i, \alpha_i, c_i, s_i, r_i)\}_{i=1}^{K}$ current set of 3D Gaussians; $\nabla_c^i \mathcal{L}$ accumulated color gradient for $G_i$; $T_c$ densification threshold

**for** $i \leftarrow 1$ **to** $K$ **do** *run in parallel*
  **if** $\nabla_c^i \mathcal{L} > T_c$ **then**
    run structured densification on $G_i$ as $\tilde{\mathcal{G}} = \text{StructDensify}(G_i)$;
    update $\mathcal{G}$ as $\mathcal{G} = \mathcal{G} \cup \tilde{\mathcal{G}} \setminus \{G_i\}$;
**end**
**return** $\mathcal{G}$

**Algorithm 2: Structured Densification** (StructDensify)

**Input:** $G(\mu, \alpha, c, s, r)$ target Gaussian to be densified

**for** $i \leftarrow 1$ **to** $K = 9$ **do** *run in parallel*
  compute placement location $\mu_i$ of the $i$-th new Gaussian; `// line 181`
  initialize $\alpha_i$, $c_i$, $s_i$, $r_i$ from $\alpha$, $c$, $s/8$, $r$;
  initialize $G_i$ as $G_i(\alpha_i, c_i, s_i, r_i)$;
**end**
**return** $\{G_i\}_{i=1}^{9}$

Figure 12: Algorithms of the proposed ReGS.

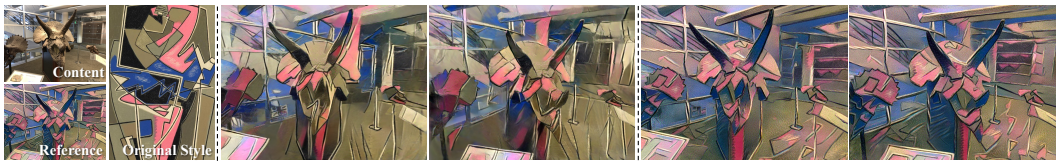


(a) SNeRF with the original style image (b) ReGS with the reference

Figure 13: Visual comparison on aesthetic quality with SNeRF (using original style image).

achieve peak performance but also without inducing many excessive Gaussians that might slow down rendering.

### C.4 Additional Loss Components

ReGS adopts TCM and color matching loss from [10] to spread textures to occluded areas. Here we re-assess their effectiveness for 3DGS. As shown in Figure 11, using color matching loss reduces color mismatch and using TCM loss removes artifacts in the occluded areas. These findings are similar to the observations in [10]. These results suggest that the adopted losses indeed work for our 3DGS-based model.

## D Limitations and Future Work

With ReGS, one can achieve real-time stylized view synthesis at high quality. However, it cannot significantly improve the training efficiency over previous methods [10, 8, 4], when adapting to a novel style reference. During training, efficiency bottleneck comes from the feature extraction and matching steps in $\mathcal{L}_{TCM}$, which is significantly slower than the splatting rendering [11]. Therefore, using 3DGS as scene representation cannot benefit much for the training efficiency. On the other hand, arbitrary stylization methods [9, 6] have made possible for adapting to a novel style in a zero-short manner with reasonable good performance. Following their spirit, designing a universal 3D Gaussian stylizer that can generalize to any references without run-time optimization might be an interesting direction for further improving training efficiency.

Moreover, beside editing the appearance, further styling geometry can be another interesting future direction. ReGS might be able to handle minor shape changes, for example, by relaxing the depth supervision. However, precise geometry editing based on a reference image is inherently more challenging due to single-view shape ambiguity. To achieve high-quality geometry stylization, existing methods often adopt a very different set of techniques such as shape prior [104], text guidance [105] and/or generative modeling [88, 90, 89] to hallucinate missing geometry. Combining our method with these techniques for joint geometry and appearance editing is an open and interesting future direction.

## E Additional Comparison on Aesthetic Quality

In Figure 13, we provide additional comparisons on aesthetic quality with SNeRF [4], by providing the original 2D art image. One can see that SNeRF produces results mimicking the abstract style of

https://doi.org/10.52202/079017-0132


Figure 14: More visual comparison results. Our method can faithfully reproduce the texture in reference image.


https://doi.org/10.52202/079017-0132

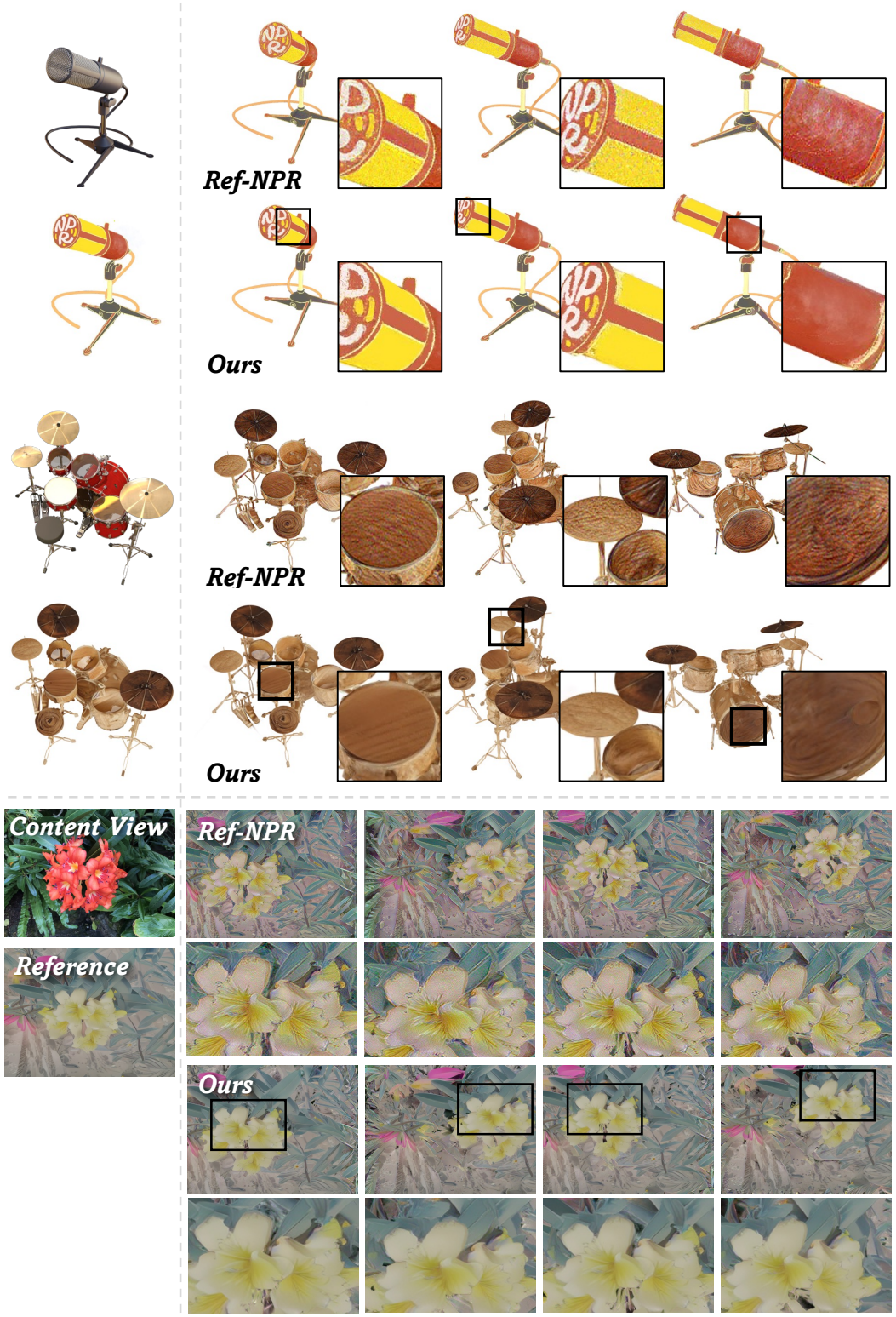


Figure 15: More visual comparison results with Ref-NPR [10]. Our method faithfully reproduce the texture in reference image. In contrast, Ref-NPR [10] produces images with lower quality.

Figure 16: Stylization results of multiple style references on a single baked scene.

Table 2: Detailed Ref-LPIPS results on each scene

| Method | Chair | Ficus | Hotdog | Mic | Flower | Horn | Truck | Playground | Average |
|---|---|---|---|---|---|---|---|---|---|
| ARF | 0.185 | 0.123 | 0.300 | 0.146 | 0.619 | 0.502 | 0.683 | 0.592 | 0.394 |
| SNeRF | 0.188 | 0.129 | 0.283 | 0.138 | 0.646 | 0.492 | 0.702 | 0.663 | 0.405 |
| Ref-NPR | 0.164 | 0.122 | 0.273 | 0.126 | 0.289 | 0.471 | 0.669 | 0.596 | 0.339 |
| ReGS | **0.127** | **0.119** | **0.175** | **0.104** | **0.134** | **0.367** | **0.454** | **0.472** | **0.202** |

the original art, whereas our method follows the extract stylized texture in the reference image by design.

## F More Results

We present more visual comparison results in Figure 14 & 15 to better demonstrate the superiority of our approach. In Figure 16, we show results of multiple style references acting on a single baked scene. In Table 2, we report Ref-LPIPS score of each scene. Our method consistently outperforms baselines.


https://doi.org/10.52202/079017-0132

## NeurIPS Paper Checklist

1. **Claims**

   Question: Do the main claims made in the abstract and introduction accurately reflect the paper's contributions and scope?

   Answer: [Yes]

   Justification: Content of this manuscript is organized following abstract and introduction.

   Guidelines:

   - The answer NA means that the abstract and introduction do not include the claims made in the paper.
   - The abstract and/or introduction should clearly state the claims made, including the contributions made in the paper and important assumptions and limitations. A No or NA answer to this question will not be perceived well by the reviewers.
   - The claims made should match theoretical and experimental results, and reflect how much the results can be expected to generalize to other settings.
   - It is fine to include aspirational goals as motivation as long as it is clear that these goals are not attained by the paper.

2. **Limitations**

   Question: Does the paper discuss the limitations of the work performed by the authors?

   Answer: [Yes]

   Justification: See the supplemental file.

   Guidelines:

   - The answer NA means that the paper has no limitation while the answer No means that the paper has limitations, but those are not discussed in the paper.
   - The authors are encouraged to create a separate "Limitations" section in their paper.
   - The paper should point out any strong assumptions and how robust the results are to violations of these assumptions (e.g., independence assumptions, noiseless settings, model well-specification, asymptotic approximations only holding locally). The authors should reflect on how these assumptions might be violated in practice and what the implications would be.
   - The authors should reflect on the scope of the claims made, e.g., if the approach was only tested on a few datasets or with a few runs. In general, empirical results often depend on implicit assumptions, which should be articulated.
   - The authors should reflect on the factors that influence the performance of the approach. For example, a facial recognition algorithm may perform poorly when image resolution is low or images are taken in low lighting. Or a speech-to-text system might not be used reliably to provide closed captions for online lectures because it fails to handle technical jargon.
   - The authors should discuss the computational efficiency of the proposed algorithms and how they scale with dataset size.
   - If applicable, the authors should discuss possible limitations of their approach to address problems of privacy and fairness.
   - While the authors might fear that complete honesty about limitations might be used by reviewers as grounds for rejection, a worse outcome might be that reviewers discover limitations that aren't acknowledged in the paper. The authors should use their best judgment and recognize that individual actions in favor of transparency play an important role in developing norms that preserve the integrity of the community. Reviewers will be specifically instructed to not penalize honesty concerning limitations.

3. **Theory Assumptions and Proofs**

   Question: For each theoretical result, does the paper provide the full set of assumptions and a complete (and correct) proof?

   Answer: [NA]

Justification: This manuscript is not a theory paper.

Guidelines:

- The answer NA means that the paper does not include theoretical results.
- All the theorems, formulas, and proofs in the paper should be numbered and cross-referenced.
- All assumptions should be clearly stated or referenced in the statement of any theorems.
- The proofs can either appear in the main paper or the supplemental material, but if they appear in the supplemental material, the authors are encouraged to provide a short proof sketch to provide intuition.
- Inversely, any informal proof provided in the core of the paper should be complemented by formal proofs provided in appendix or supplemental material.
- Theorems and Lemmas that the proof relies upon should be properly referenced.

4. **Experimental Result Reproducibility**

   Question: Does the paper fully disclose all the information needed to reproduce the main experimental results of the paper to the extent that it affects the main claims and/or conclusions of the paper (regardless of whether the code and data are provided or not)?

   Answer: [Yes]

   Justification: Implementation details are provided.

   Guidelines:

   - The answer NA means that the paper does not include experiments.
   - If the paper includes experiments, a No answer to this question will not be perceived well by the reviewers: Making the paper reproducible is important, regardless of whether the code and data are provided or not.
   - If the contribution is a dataset and/or model, the authors should describe the steps taken to make their results reproducible or verifiable.
   - Depending on the contribution, reproducibility can be accomplished in various ways. For example, if the contribution is a novel architecture, describing the architecture fully might suffice, or if the contribution is a specific model and empirical evaluation, it may be necessary to either make it possible for others to replicate the model with the same dataset, or provide access to the model. In general. releasing code and data is often one good way to accomplish this, but reproducibility can also be provided via detailed instructions for how to replicate the results, access to a hosted model (e.g., in the case of a large language model), releasing of a model checkpoint, or other means that are appropriate to the research performed.
   - While NeurIPS does not require releasing code, the conference does require all submissions to provide some reasonable avenue for reproducibility, which may depend on the nature of the contribution. For example
     (a) If the contribution is primarily a new algorithm, the paper should make it clear how to reproduce that algorithm.
     (b) If the contribution is primarily a new model architecture, the paper should describe the architecture clearly and fully.
     (c) If the contribution is a new model (e.g., a large language model), then there should either be a way to access this model for reproducing the results or a way to reproduce the model (e.g., with an open-source dataset or instructions for how to construct the dataset).
     (d) We recognize that reproducibility may be tricky in some cases, in which case authors are welcome to describe the particular way they provide for reproducibility. In the case of closed-source models, it may be that access to the model is limited in some way (e.g., to registered users), but it should be possible for other researchers to have some path to reproducing or verifying the results.

5. **Open access to data and code**

   Question: Does the paper provide open access to the data and code, with sufficient instructions to faithfully reproduce the main experimental results, as described in supplemental material?


https://doi.org/10.52202/079017-0132

Answer: [Yes]

Justification: Code will be released before the conference.

Guidelines:

- The answer NA means that paper does not include experiments requiring code.
- Please see the NeurIPS code and data submission guidelines (`https://nips.cc/public/guides/CodeSubmissionPolicy`) for more details.
- While we encourage the release of code and data, we understand that this might not be possible, so "No" is an acceptable answer. Papers cannot be rejected simply for not including code, unless this is central to the contribution (e.g., for a new open-source benchmark).
- The instructions should contain the exact command and environment needed to run to reproduce the results. See the NeurIPS code and data submission guidelines (`https://nips.cc/public/guides/CodeSubmissionPolicy`) for more details.
- The authors should provide instructions on data access and preparation, including how to access the raw data, preprocessed data, intermediate data, and generated data, etc.
- The authors should provide scripts to reproduce all experimental results for the new proposed method and baselines. If only a subset of experiments are reproducible, they should state which ones are omitted from the script and why.
- At submission time, to preserve anonymity, the authors should release anonymized versions (if applicable).
- Providing as much information as possible in supplemental material (appended to the paper) is recommended, but including URLs to data and code is permitted.

6. **Experimental Setting/Details**

   Question: Does the paper specify all the training and test details (e.g., data splits, hyperparameters, how they were chosen, type of optimizer, etc.) necessary to understand the results?

   Answer: [Yes]

   Justification: Experiment settings and implementation details are provided in Section 3.6.

   Guidelines:

   - The answer NA means that the paper does not include experiments.
   - The experimental setting should be presented in the core of the paper to a level of detail that is necessary to appreciate the results and make sense of them.
   - The full details can be provided either with the code, in appendix, or as supplemental material.

7. **Experiment Statistical Significance**

   Question: Does the paper report error bars suitably and correctly defined or other appropriate information about the statistical significance of the experiments?

   Answer: [No]

   Justification: Our method is statistically stable.

   Guidelines:

   - The answer NA means that the paper does not include experiments.
   - The authors should answer "Yes" if the results are accompanied by error bars, confidence intervals, or statistical significance tests, at least for the experiments that support the main claims of the paper.
   - The factors of variability that the error bars are capturing should be clearly stated (for example, train/test split, initialization, random drawing of some parameter, or overall run with given experimental conditions).
   - The method for calculating the error bars should be explained (closed form formula, call to a library function, bootstrap, etc.)
   - The assumptions made should be given (e.g., Normally distributed errors).
   - It should be clear whether the error bar is the standard deviation or the standard error of the mean.

- It is OK to report 1-sigma error bars, but one should state it. The authors should preferably report a 2-sigma error bar than state that they have a 96% CI, if the hypothesis of Normality of errors is not verified.
- For asymmetric distributions, the authors should be careful not to show in tables or figures symmetric error bars that would yield results that are out of range (e.g. negative error rates).
- If error bars are reported in tables or plots, The authors should explain in the text how they were calculated and reference the corresponding figures or tables in the text.

8. **Experiments Compute Resources**

   Question: For each experiment, does the paper provide sufficient information on the computer resources (type of compute workers, memory, time of execution) needed to reproduce the experiments?

   Answer: [Yes]

   Justification: See section 3.6.

   Guidelines:

   - The answer NA means that the paper does not include experiments.
   - The paper should indicate the type of compute workers CPU or GPU, internal cluster, or cloud provider, including relevant memory and storage.
   - The paper should provide the amount of compute required for each of the individual experimental runs as well as estimate the total compute.
   - The paper should disclose whether the full research project required more compute than the experiments reported in the paper (e.g., preliminary or failed experiments that didn't make it into the paper).

9. **Code Of Ethics**

   Question: Does the research conducted in the paper conform, in every respect, with the NeurIPS Code of Ethics `https://neurips.cc/public/EthicsGuidelines`?

   Answer: [Yes]

   Justification: The research conforms with the the NeurIPS Code of Ethics.

   Guidelines:

   - The answer NA means that the authors have not reviewed the NeurIPS Code of Ethics.
   - If the authors answer No, they should explain the special circumstances that require a deviation from the Code of Ethics.
   - The authors should make sure to preserve anonymity (e.g., if there is a special consideration due to laws or regulations in their jurisdiction).

10. **Broader Impacts**

    Question: Does the paper discuss both potential positive societal impacts and negative societal impacts of the work performed?

    Answer: [Yes]

    Justification: We discussed the potential applications of this work. This paper does not have apparent negative societal impact.

    Guidelines:

    - The answer NA means that there is no societal impact of the work performed.
    - If the authors answer NA or No, they should explain why their work has no societal impact or why the paper does not address societal impact.
    - Examples of negative societal impacts include potential malicious or unintended uses (e.g., disinformation, generating fake profiles, surveillance), fairness considerations (e.g., deployment of technologies that could make decisions that unfairly impact specific groups), privacy considerations, and security considerations.


https://doi.org/10.52202/079017-0132

- The conference expects that many papers will be foundational research and not tied to particular applications, let alone deployments. However, if there is a direct path to any negative applications, the authors should point it out. For example, it is legitimate to point out that an improvement in the quality of generative models could be used to generate deepfakes for disinformation. On the other hand, it is not needed to point out that a generic algorithm for optimizing neural networks could enable people to train models that generate Deepfakes faster.
- The authors should consider possible harms that could arise when the technology is being used as intended and functioning correctly, harms that could arise when the technology is being used as intended but gives incorrect results, and harms following from (intentional or unintentional) misuse of the technology.
- If there are negative societal impacts, the authors could also discuss possible mitigation strategies (e.g., gated release of models, providing defenses in addition to attacks, mechanisms for monitoring misuse, mechanisms to monitor how a system learns from feedback over time, improving the efficiency and accessibility of ML).

11. **Safeguards**

    Question: Does the paper describe safeguards that have been put in place for responsible release of data or models that have a high risk for misuse (e.g., pretrained language models, image generators, or scraped datasets)?

    Answer: [NA]

    Justification: The paper poses no such risks.

    Guidelines:

    - The answer NA means that the paper poses no such risks.
    - Released models that have a high risk for misuse or dual-use should be released with necessary safeguards to allow for controlled use of the model, for example by requiring that users adhere to usage guidelines or restrictions to access the model or implementing safety filters.
    - Datasets that have been scraped from the Internet could pose safety risks. The authors should describe how they avoided releasing unsafe images.
    - We recognize that providing effective safeguards is challenging, and many papers do not require this, but we encourage authors to take this into account and make a best faith effort.

12. **Licenses for existing assets**

    Question: Are the creators or original owners of assets (e.g., code, data, models), used in the paper, properly credited and are the license and terms of use explicitly mentioned and properly respected?

    Answer: [Yes]

    Justification: All assets are credited in this manuscript.

    Guidelines:

    - The answer NA means that the paper does not use existing assets.
    - The authors should cite the original paper that produced the code package or dataset.
    - The authors should state which version of the asset is used and, if possible, include a URL.
    - The name of the license (e.g., CC-BY 4.0) should be included for each asset.
    - For scraped data from a particular source (e.g., website), the copyright and terms of service of that source should be provided.
    - If assets are released, the license, copyright information, and terms of use in the package should be provided. For popular datasets, `paperswithcode.com/datasets` has curated licenses for some datasets. Their licensing guide can help determine the license of a dataset.
    - For existing datasets that are re-packaged, both the original license and the license of the derived asset (if it has changed) should be provided.

- If this information is not available online, the authors are encouraged to reach out to the asset's creators.

13. **New Assets**

    Question: Are new assets introduced in the paper well documented and is the documentation provided alongside the assets?

    Answer: [NA]

    Justification: The paper does not release new assets.

    Guidelines:

    - The answer NA means that the paper does not release new assets.
    - Researchers should communicate the details of the dataset/code/model as part of their submissions via structured templates. This includes details about training, license, limitations, etc.
    - The paper should discuss whether and how consent was obtained from people whose asset is used.
    - At submission time, remember to anonymize your assets (if applicable). You can either create an anonymized URL or include an anonymized zip file.

14. **Crowdsourcing and Research with Human Subjects**

    Question: For crowdsourcing experiments and research with human subjects, does the paper include the full text of instructions given to participants and screenshots, if applicable, as well as details about compensation (if any)?

    Answer: [NA]

    Justification: The paper does not involve crowdsourcing nor research with human subjects.

    Guidelines:

    - The answer NA means that the paper does not involve crowdsourcing nor research with human subjects.
    - Including this information in the supplemental material is fine, but if the main contribution of the paper involves human subjects, then as much detail as possible should be included in the main paper.
    - According to the NeurIPS Code of Ethics, workers involved in data collection, curation, or other labor should be paid at least the minimum wage in the country of the data collector.

15. **Institutional Review Board (IRB) Approvals or Equivalent for Research with Human Subjects**

    Question: Does the paper describe potential risks incurred by study participants, whether such risks were disclosed to the subjects, and whether Institutional Review Board (IRB) approvals (or an equivalent approval/review based on the requirements of your country or institution) were obtained?

    Answer: [NA]

    Justification: The paper does not involve crowdsourcing nor research with human subjects.

    Guidelines:

    - The answer NA means that the paper does not involve crowdsourcing nor research with human subjects.
    - Depending on the country in which research is conducted, IRB approval (or equivalent) may be required for any human subjects research. If you obtained IRB approval, you should clearly state this in the paper.
    - We recognize that the procedures for this may vary significantly between institutions and locations, and we expect authors to adhere to the NeurIPS Code of Ethics and the guidelines for their institution.
    - For initial submissions, do not include any information that would break anonymity (if applicable), such as the institution conducting the review.


https://doi.org/10.52202/079017-0132